HHS Public Access

Author manuscript

Eur J Immunol. Author manuscript; available in PMC 2020 January 10.

Published in final edited form as:

Eur J Immunol. 2019 March ; 49(3): 428–442. doi:10.1002/eji.201847789.

IL-4 promotes stromal cell expansion and is critical for development of a type-2, but not a type 1 immune response

Diana Cortes-Selva[1], **Andrew Ready**[1], **Lisa Gibbs**[3], **Bartek Rajwa**[2], **Keke C. Fairfax**[1,3]

[1]Department of Comparative Pathobiology, College of Veterinary Medicine, Purdue University, West Lafayette, IN, USA

[2]Department of Basic Medical Sciences College of Veterinary Medicine, and Bindley Biosciences Center, Purdue University, West Lafayette, IN, USA

[3]Department of Pathology, Division of Microbiology and Immunology, University of Utah School of Medicine, Salt Lake City, UT, USA

Abstract

IL-4 is critical for differentiation of Th2 cells and antibody isotype switching, but our work demonstrated that it is produced in the peripheral LN under both Type 2, and Type 1 conditions, raising the possibility of other functions. We found that IL-4 is vital for proper positioning of hematopoietic and stromal cells in steady state, and the lack of IL-4 or IL-4Rα correlates with disarrangement of both follicular dendritic cells and $CD31^+$ endothelial cells. We observed a marked disorganization of B cells in these mice, suggesting that the lymphocyte-stromal cell axis is maintained by the IL-4 signaling pathway. This study showed that absence of IL-4 correlates with significant downregulation of Lymphotoxin alpha (LTα) and Lymphotoxin beta (LTβ), critical lymphokines for the development and maintenance of lymphoid organs. Moreover, immunization of IL-4 deficient mice with Type 2 antigens failed to induce lymphotoxin production, LN reorganization, or germinal center formation, while this process is IL-4 independent following Type 1 immunization. Additionally, we found that Type 1 antigen mediated LN reorganization is dependent on IFN-γ in the absence of IL-4. Our findings reveal a role of IL-4 in the maintenance of peripheral lymphoid organ microenvironments during homeostasis and antigenic challenge.

Keywords

cytokine; IL-4; humoral immunity; LN organization; stromal cells

Introduction

Secondary lymphoid organs (SLOs) are essential for the development of immune responses; they are responsible for facilitating pathogen and lymphocyte interactions in order to mount

Full correspondence: Dr. Keke Fairfax, Department of Pathology, Division of Microbiology and Immunology, University of Utah, JMRB 2200B, 15 N Medical Drive East, Salt Lake City, UT 84112, USA Fax: +801-581-5980 keke.fairfax@path.utah.edu.

Conflict of Interest: The authors declare no financial or commercial conflict of interest.

an efficient anti-pathogen response, and for supplying different immune-modulatory factors [1, 2]. The functions mediated by SLOs rely heavily on the structural organization of the different microenvironments. The complex micro-architecture of SLOs is characterized by the cortex (where B-cell follicles are located) and paracortex (containing the T-cell zone). In addition, an elaborate network of stromal cells provides both structural support and regulatory signals that trigger B- and T-cell migration to their respective compartments. Among these mesenchymal (stromal) cells, follicular dendritic cells (FDCs) support B-cell survival and proliferation. Previous studies have shown that FDCs produce CXCL13 to attract B cells to the B-cell follicle [3]; where they also trap immune complexes via the complement receptors CR1 (CD35) and CR2 (CD21) [4], thus rendering FDCs essential for Germinal Center (GC) formation and function. Fibroblastic reticular cells (FRC) have been reported to play an equivalent role in T cell maintenance and B-cell survival [5, 6]. FRCs express podoplanin (gp38), produce the chemokines CCL19 and CCL21, which promote the migration of CCR7 expressing cells, as well as IL-7 to promote naïve T-cell survival [7–9], and Baff to promote B-cell survival [5]. Additionally, lymphatic endothelial cells (LEC) secrete CXCL12 and CCL21 and induce recruitment of dendritic cells to the lymph node [10], and their activation by Lymphoid Tissue inducer (LTi) cells has been shown to be critical for the initiation of lymph node development [11]. Furthermore, it is well established that in lymph nodes the lymphotoxin (LT) $\alpha 1\beta 2$-LTβR pathway is important for both lymph node genesis and proper cellular organization during steady state [12–14]. Moreover, LT $\alpha 1\beta 2$ mediates the cross-talk between lymphocytes and mesenchymal-derived cells, which is required to maintain lymph node homeostasis and antigen-induced expansion [15, 16].

IL-4 is regarded as a pleiotropic cytokine and regulates maturation and survival of B cells, differentiation of Th2 lymphocytes, polarization of macrophages to the alternatively activated (M2) phenotype, and immunoglobulin isotype switching to IgG1/IgE in mice and IgG4/IgE in humans [17–19]. IL-4 is broadly produced by T cells, mast cells, basophils, eosinophils, and NKT cells [20–22]. IL-4 exerts its function by binding to type I and type II receptors. The type I receptor consists of a widely expressed IL-4Rα and a more constricted common γ-chain. IL-4Rα is expressed on T cells, B cells, eosinophils, macrophages, endothelial cells, fibroblasts, and myeloid-derived suppressor cells [23, 24]. The binding of IL-4 to IL-4R initiates a signaling cascade characterized by phosphorylation of activator of transcription factor-6 (STAT6) and transcription of IL-4 responsive genes [25]. Although IL-4, and IL-13 are considered closely related type 2 cytokines, recent reports have shown that only IL-4 is expressed in the lymph node [26, 27], which suggests a unique role of IL-4 in these organs. While previous reports on IL-4 have predominantly focused on its role in a Th2 immune response, the potential role of IL-4 in the spatial organization of peripheral lymph nodes microenvironments during homeostasis and antigenic challenge has not been explored.

Given the importance of the IL-4 signaling pathway in T and B cells, and the relevance of lymph node organization in both innate and adaptive immune responses, this study sought to explore the role of the IL-4/IL-4Rα pathway in the maintenance of LN architecture during both homeostasis and following antigenic challenge. During steady state a lack of IL-4 signaling resulted in a 50–70% reduction in FDCs and LECs and disorganization of B-cell zones. We then asked whether IL-4 was responsible for LN reorganization in response to

prototypical Type 1 (STag) and Type 2 (SEA) antigens. Interestingly, IL-4 was required for SEA induced LN reorganization, lymphotoxin production, and germinal center formation, while STag induction of these responses was IL-4 independent. Additionally, The IL-4 independent STag response was shown to be mediated at least partially by IFNγ. Finally, we asked if IL-4 is required for the development of humoral immunity in response to a Tetanus/Diphtheria commercial vaccine. Strikingly immunization of IL-4Rα deficient mice with tetanus/diphtheria failed to induce anti-diphtheria IgG1 while anti-tetanus responses were unaffected. Together, our results establish a previously unexplored role of IL-4 in the maintenance of peripheral lymphoid organ microenvironments and the induction of adaptive immunity.

Results

Maintenance of stromal cell networks in peripheral lymph nodes depends on IL-4 signaling pathway

While IL-4 is a cytokine with pleiotropic functions, [28, 29] a functional role for IL-4 in the maintenance of the microarchitecture in lymphoid organs in homeostasis has not been explored. Our previous work demonstrated that IL-4 is produced by T-follicular helper cells under both Th1 and Th2 inducing conditions [30]. To explore a potential role of IL-4 in peripheral lymph node organization we first examined lymphatic endothelial cells (LEC: $CD31^+$ $PDPN^+$ [31]), since they promote lymph node organogenesis, from IL-4 deficient mice by flow cytometry. For this purpose, we used the 4get homozygous (IL-4 GFP reporter mice bred on a BALC/c background (2)), 4get IL-4Rα deficient mice, and mice deficient in IL-4 or STAT6 on a C57BL/6J background. We observed significantly reduced frequency of LEC in mice deficient in multiple components of the IL-4 signaling pathway on both the BALB/c and C57BL/6J backgrounds (IL-$4^{-/-}$, 4getIL-4R$\alpha^{-/-}$, and STAT$6^{-/-}$), with a 50% reduction in 4getIL-$4R^{-/-}$ mice and 78% and 50% reduction in IL-$4^{-/-}$ and STAT$6^{-/-}$, respectively, compared to wild-type (Fig. 1A, B) and an effect size (calculated by Cohen's D) of 1.99, 1.39, and 3.96 in IL$4^{-/-}$, STAT$6^{-/-}$, and 4getIL-4R$\alpha^{-/-}$, respectively. Blood endothelial cell (BEC: CD31+PDPN−) and pericyte (double negative) populations were not significantly altered, while fibroblastic reticular cells (FRC: PDPN+CD31−) trended toward reduction, but the alterations were not statistically significant in any of the three strains deficient in IL-4 signaling ($p = 0.07$). Moreover, the observed reduction of LEC was limited to popliteal lymph nodes, as we did not observe any significant reduction of LEC in mesenteric lymph nodes (Data not shown). The ImmGen database indicates that LECs have *il4ralpha* transcripts, and we confirmed that they are also surface positive for IL-4Rα compared to 4getIL-4R$\alpha^{-/-}$ mice (Fig. 1D). We then quantified the gene expression levels of *CCL19* and *CCL21*, which are both secreted by FRC to induce lymph node entry of lymphocytes, and observed no significant change in fold expression (Fig. 1E, F). Next, we evaluated the localization of these stromal cells in the popliteal lymph node using tile confocal microscopy. Lymphatic endothelial cells are characterized in the lymph node by expression of markers such as pdpn (gp38), CD31, and their location. LEC localize at the subcapsular sinus and come in contact with subcapsular macrophages [32,33]. LEC then ramify to the cortex and into the T-cell zone and connect to the medulla at the exit of the lymph node. In homeostasis, these cell networks have a distinct structure characterized by

abundant invaginations that are interconnected by several junctions; we analyzed the distribution of $CD31^+$ and $PDPN^+$ endothelial cells and observed a marked mislocalization in 4getIL-4Rα$^{-/-}$ compared to wild-type controls. In the lymph node of wild-type mice, $CD31^+$ cells were distributed along the subcapsular sinus, the border of the cortex, and throughout the T-cell zone, consistent with previous reports of their steady-state distribution [34, 35] (Fig. 1 H). In contrast, our mice deficient in IL-4Rα exhibited a collapsed phenotype, with overall less CD31 staining and concentrated clusters of $CD31^+$ cells constrained within the medulla, suggesting a requirement of IL-4 for the localization of cortical LECs in the inactivated peripheral lymph node. In order to quantify the spatial distribution of costained CD31 and podoplanin, we used analysis of locally bright features (LBF [36]) (Supporting Information Fig. 2) and observed that LBF in WT were localized near the boundaries the region of interest (ROI), whereas the IL-4RαKO trended toward a higher proportion of LBF localized further from the ROI suggesting an altered distribution in the lymph node. We also stained with ICAM-2, a key cellular adhesion molecule involved in lymphocyte recruitment into the lymph node [37], in wild-type mice ICAM-2 colocalized with many $CD31^+$ structures in the subcapsular and cortex regions. In contrast, 4getIL-4Rα$^{-/-}$ mice have ICAM-2^+ cells in the collapsed $CD31^+$ structures in the medulla, with many cells also staining positive for PDPN (Fig. 1G). Altered distribution of LEC populations did not lead to $CD4^+$ T-cell frequencies, but we did observe reduction in T-cell number in the IL-4 deficient animals, but not in the STAT6$^{-/-}$ or the 4getIL-4Rα$^{-/-}$ mice (Supporting Information Fig. 1A, B). High endothelial venules (HEV) are responsible for lymphocyte migration to the lymph node [38]. To confirm that disorganization is not driven by a defect in HEV-mediated migration, we analyzed $PNAd^+$ HEV and found no alterations to PNAd localization in 4getIL-4Rα$^{-/-}$ mice, indicating that the lack of IL-4 signaling does not alter high endothelial venules (Supporting Information Fig. 1E).

IL-4 signaling is critical for proper follicular dendritic cell positioning in the lymph node

FDC express CXCL13 and capture and present opsonized antigens to B cells [39, 40]. MFG-E8 (suggested to be identical to FDC marker, FDC-M1) and FDC-M2 (activated C4, [41]) are highly expressed in this cell population and in primary and secondary follicles and are considered specific molecular markers of FDC. In addition, FDC are recognized by antibodies to the complement receptors CD21 and CD35 (37). In our experiments, we observed a significant decrease in the frequency and cell numbers of FDC-$M2^+$ $CD21/35^+$ FDC cells in mice lacking the IL-4 signaling cascade (IL-4$^{-/-}$, 4get/IL-4Rα$^{-/-}$, and STAT6$^{-/-}$) on both the C57BL/6J and BALB/c genetic backgrounds (Fig. 2B,C). As with LECs, the bulk population of FDCs is surface positive for IL-4Rα (Fig. 2D). As FDCs have previously been reported to maintain B-cell area via CXCL13 [39], we investigated the CXCL13 gene expression in peripheral lymph nodes of 4getIL-4R$^{-/-}$ mice, and observed no alterations (Fig. 2E). Using tile confocal microscopy, we observed clusters of FDC-$M2^+$ and $CD21/35^+$ cells on the edges of the B-cell zones in 4get homozygous mice, as expected. We also observed B-cell follicle mislocalization in IL-4Rα deficient mice, with B-cell follicles localized further from capsule in compared to wild type (Fig. 2F, G, and I). B-cell follicle mislocalization was not related to change in cell number, as we observed no significant difference in frequencies or cell number on either the BALB/c or C57BL/6J background (Supporting Information Fig. 1B, 1D). The IL-4Rα deficient mice on the other hand,

displayed distinctly altered localization of FDCs (characterized as FDC-M2$^+$ in Fig. 2F and CD21/35$^+$ in Fig. 2G), with B cells clustering around the aberrantly positioned FDCs. Moreover, we analyzed the spatial positioning of CD21/35+ FDC by quantification of distance to capsule (normalized to the total area of the LN) and observed significant alterations in the positioning of FDC in the IL-4RαKO mice in comparison to wild type controls (Fig. 2 H). Interestingly, FDCs and B cells were consistently found clustered together, since bulk CXCL13 expression is unaltered, it suggests that IL-4 mediated positioning is independent of CXCL13. These data suggest that the stromal-lymphocyte organizational axis [42, 43] is compromised in mice in which the IL-4 signaling pathway is deficient in some of its components, a state that could potentially lead to a deficiency in the B-cell response to antigenic challenge.

Deficiency of IL-4 correlates with downregulation of lymphotoxin β and lymphotoxin α gene expression

During homeostasis, the development and regulation of diverse lymphoid tissue microenvironments is tightly related to expression of lymphotoxin. Mice deficient in LTα, LTβ, and LTβR all present defects in lymphoid organogenesis, showing the remarkable dependence of lymphoid homeostasis on the LTα1β2-LTβR signaling axis [44]. In addition, BAFF (known as BlyS, TALL-1, TNFSF13B, TNFSF20) is secreted by FRCs and FDCs and also plays a role in the maintenance of LN architecture by aiding in the viability of B cells [5]. We investigated whether the disorganization observed in peripheral lymphoid organs could be due to defects in the LTα1β2-LTβR signaling pathway, or BAFF. For this, we first tested the gene expression of *lt*β and *lta* in mice lacking IL-4Rα or the transcription factor Stat6. Remarkably, absence of IL-4Rα correlated to significant decrease in both *lt*α and *lt*β gene expression. Nevertheless, mRNA expression of *baff* in the lymph node was unaffected in the absence of IL-4R*a* (Fig. 3A). Similarly, we also tested the gene expression of *lt*β and *lt*α in popliteal lymph nodes extracted from C57BL/6J mice, IL-4$^{-/-}$, and in STAT6$^{-/-}$ mice; we observed significantly reduced gene expression of *lt*α and *lt*β, but not *baff* in the STAT6$^{-/-}$ and IL-4$^{-/-}$ animals (Fig. 3B, C). Furthermore, protein expression of LTβ was also downregulated in IL-4R deficient and STAT6 knockout mice compared to their respective wild types (Fig. 3D, E). These data suggest that IL-4 may act in an IL-4R and Stat-6 dependent manner to sustain LTα/β production, but is not involved in regulating BAFF.

IL-4 is required for LN reorganization and GC formation in a Type-2 but not a Type-1 response

The organization and expansion of B and T cells in lymph nodes following antigenic stimulation is closely related to the complex stromal cell network [42], therefore we wondered if the disorganization observed in stromal cells from peripheral lymph nodes affected the adaptive immune response to the parasitic antigens of *Schistosoma mansoni* (SEA, which induces a Type 2 response), and *Toxoplasma gondii* antigen (STag, which induces a Type 1 response).

To determine whether IL-4 deficiency affected the expansion of T-follicular helper cells (defined as CD4$^+$CXCR5$^+$PD-1$^+$) in peripheral lymph nodes we injected the footpad of

IL-4$^{-/-}$ mice and C57BL/6 mice with unadjuvanted SEA and STag. Similar to what we have previously published [30], immunization with SEA resulted in reduced Tfh in IL-4$^{-/-}$ (but with no reduction in Tfh cell function as measured by IL-21 production, Fig. 4B) and plasma cells, as compared to wild type controls at 8-days post-immunization (Fig. 4A, C). While the lack of IL-4 did not lead to diminished Tfh or plasma cells following STag immunization (Fig. 4A, C). As expected, IL-4$^{-/-}$ mice immunized with either SEA or STag had significantly reduced production of IgG1 (Supporting Information Fig. 3B). Given that Tfh cells have been shown to be positional-dependent cells [45], we investigated the role of IL-4 in the organization of these cells in the lymph node. We imaged B- and T-cell zones as well as germinal centers in fresh-frozen sections of reactive lymph nodes at day 8 postimmunization. Naïve IL-4 deficient mice showed the characteristic disorganization of B-cell follicles as observed in Fig. 2 (Fig. 4D), with B220 positive cells distributed along the paracortex, cortex, and medulla, as well as a loss of defined B-cell follicles. Mice immunized with SEA also showed a marked disorganization of the B-cell follicles and T-cell zone, with B-cell clusters appearing throughout the T-cell zone and no apparent organized GL7-positive germinal centers (Fig. 4E), whereas mice immunized with STag showed organization and germinal center localization similar to the wild type control (Fig. 4F). The analysis of spatial positioning of B220^{+} cells by quantification of distance to capsule (normalized to the total area of the LN) showed that IL-4 knockout mice at both steady state, and immunized with SEA antigens have B-cell follicles localized significantly further from capsule in comparison to wild type, whereas IL-4 knockout mice immunized with STag exhibit similar localization of B-cell follicles from the capsule when compared to wild type controls (Fig. 4G). Since we identified defects in lymphotoxin expression at steady state in the absence of IL-4 signaling, we assessed the ability of SEA and STag to induce *lt*β and *lt*α gene expression in the absence of IL-4. SEA immunization of IL-4$^{-/-}$ mice induced significantly less *lt*β and *lt*α expression as compared to wild type mice, while STag immunization induced equal transcripts levels of *lt*β and *lt*α in wild type and IL-4$^{-/-}$ animals (Fig. 4H and I), suggesting that there is an IL-4 independent mechanism for lymph node reorganization during a Type 1 immune response.

IFNγ mediates LEC expansion in the absence of IL-4

Our data indicate that STag immunization is able to induce lymphotoxin production and lymph node reorganization in the absence of IL-4. Since we have previously shown that STag induces significantly more IFNγ expression than SEA does [30], we wondered if IFNγ production is the mechanism through which STag is able to stimulate LEC and FDC expansion and lymph node reorganization independently of IL-4. To examine this possibility, we administered blocking anti-IFNγ mAb or isotype control to 4get and 4getIL-4Rα$^{-/-}$ mice (4getIL-4Rα$^{-/-}$ have significantly reduced FDCs and LEC at steady state, Figs. 1 and 2) beginning at three days before immunization with STag (Fig. 5A). At day 8 post-immunization, isotype control treated STag immunized 4get and 4get IL-4Rα$^{-/-}$ mice have equivalent cell numbers of LECs (Fig. 5B, $p = 0.1299$) and FDCs (Fig. 5C, $p = 0.3841$), suggesting that STag immunization induces expansion of these populations in 4get IL-4Rα$^{-/-}$ mice. Anti-IFNγ mAb treatment leads to significantly fewer LECs in 4get IL-4Rα$^{-/-}$ and in control 4get mice (Fig. 5B), indicating that STag induced expansion of lymphatic endothelial cells is at least partially IFNγ-dependent in the absence of IL-4Rα

signaling. Anti-IFNγ mAb treatment significantly reduced the frequency and number of FDCs in control 4get, but only reduced FDC frequency in 4get IL-4Rα$^{-/-}$ mice (Fig. 5C), suggesting that in the absence of IL-4, FDC expansion is not significantly dependent on IFN-γ and that the two stromal cell populations have different requirements for T-cell derived cytokines.

IL-4 is required for the development of a humoral immune response to tetanus/diphtheria vaccination

Our experiments with SEA as a model Type 2 antigenic challenge suggested that the development of type 2 immunity is compromised in the absence of IL-4 signaling. Since the majority of commercially available vaccines rely on alum as an adjuvant, we sought to determine if this observation has consequences for the development of humoral immunity to tetanus/diphtheria. To address this, we immunized 4get (IL-4 GFP reporter mice) and 4getIL-4Rα$^{-/-}$ mice s.c. with 1/10 the human dose of tetanus/diphtheria. We have previously established that the peak of the Tfh-cell response (to both Th1 and Th2 antigens [30]) occurs at day 8-post-immunization, therefore we assessed Tfh cell populations and IL-4 secretion at day 8 post-immunization. At this time-point 4getIL-4Rα$^{-/-}$ mice have a 60% reduction in the frequency of Tfh cells and a 70% reduction in GFP^{+} Th2 cells accompanied by a significant reduction in cell number (Fig. 6A, B) compared to wild type 4get mice. We next explored the B-cell response at day 14 (the peak of the germinal B-cell reaction under both Th1 and Th2 conditions). At this time-point the early loss of Tfh cells is accompanied by a 60–70% reduction in germinal center and plasma cells in tetanus/diphtheria immunized IL-4Rα deficient mice (Fig. 6C, D). We then examined the stromal cell compartment to see if tetanus/diphtheria is able to expand the FDC and LEC populations. Immunized 4getIL-4Rα$^{-/-}$ have a significant reduction in the frequency and cell numbers of both LECs and FDCs ($p = 0.0093$ and $p = 0.0217$, Fig. 6E, F) compared to immunized 4get control mice. Interestingly, in absence of IL-4, the antibody response to diphtheria is significantly compromised at both days 8 and 14 post-immunization, whereas the response to tetanus is not (Fig. 6G–J), suggesting that diphtheria has a requirement for IL-4 that is similar to that of SEA. In order to rule out the possibility that impaired Tfh response and humoral responses resulted from intrinsic defects of IL-4R in these cell populations, we analyzed the Mesenteric Lymph Node (MLN) following tetanus/diphtheria immunization, and observed no differences in CD31^{+}PDPN^{+} LEC in IL-4Rα deficient mice in comparison to wild type control (Supporting Information Fig. 4).

Together, these data suggest that alum induced cellular and humoral immunity to certain antigens is compromised in the absence of IL-4 signaling, a finding that correlates to impaired expansion of certain stromal cell population in the lymph node, and has significant translational implications.

Discussion

IL-4 is known to have critical effector and homeostatic effects on lymphocytes, including protecting B cells from apoptosis, inducing IgG1 and IgE production, polarization of CD4^{+} T cells to a Th2 phenotype. For nonlymphocytes, it has been recently suggested that IL-4

acts directly on human mesenchymal progenitors and down-regulates gp38 on stromal cells lines, acting as a B-cell extrinsic mechanism to modulate the Tfh/Tfh-like- stroma crosstalk in follicular lymphoma [46]. Given the relevance of lymphocyte and stromal cell population in lymphoid organs, we sought to determine the function of IL-4 in peripheral lymph nodes. In the lymph node, IL-4 is recognized primarily as a type 2 cytokine that regulates antibody class-switching. Here, we provide evidence that IL-4 production also functions to maintain peripheral lymph node architecture in steady state, and drives antigen induced lymph node expansion. Specifically, we found that mice deficient in the IL-4 signaling cascade have an altered distribution of B-cell follicles, with reduced FDCs and LECs both in steady state and following type 2 antigenic challenge. Our data, from multiple strains of mice deficient in components of the IL-4 signaling pathway, demonstrate that IL-4 supports lymph node lymphotoxin production in steady state, a key lymphokine known to be critical for maintaining the lymphocyte-stromal cell axis. To our knowledge, this is the first report of a role for IL-4 in lymph node homeostasis.

C57BL/6J mice are recognized to have an immune skewing toward IFNγ production and strong type-1 immune responses while BALB/c mice produce more IL-4 and are skewed toward strong type 2 responses, characteristics that affect susceptibility/resistance to multiple pathogens [47, 48]. This skewing raised the possibility that IL-4 could have strain-specific homeostatic effects. To ensure the broad applicability of our findings we used mice on both BALB/c and C57BL/6J backgrounds. IL-4, IL-4Rα, and Stat-6 deficient mice from both genetic backgrounds all have profound alterations in both the frequency and cell number of LECs, and the positioning of $PDPN^+$ and $CD31^+$ structures within the peripheral lymph node (Fig. 1B, C, G). LECs have previously been reported to be dependent on lymphotoxin β receptor during inflammatory lymphangiogenesis [49], so, our findings that they express IL-4Rα on their surface, and that IL-$4^{-/-}$, 4getIL-4R$\alpha^{-/-}$, and Stat$6^{-/-}$ mice all have reduced transcripts of both LTα and LTβ, suggests that the effects of IL-4 deficiency may be due in part to altered production of these key cytokines. Helminth infection has been previously shown to induce fibroblastic reticular cell driven de novo B-cell follicle formation in the MLN via an IL-4Rα dependent induction of lymphotoxin [50]. Those experiments did not find a defect in MLN lymph node organization in IL-4R$\alpha^{-/-}$ at steady state, but the authors did not examine peripheral lymph nodes. We have examined the mesenteric lymph nodes of both IL-$4^{-/-}$ and 4getIL-4R$\alpha^{-/-}$ mice and have not observed the same disorganization that we have found in peripheral lymph nodes (Supporting Information Fig. 1 and data not shown), suggesting that homeostatic cytokine signals are distinct in different lymphoid organs, as has been previously suggested by other groups. Previous work has demonstrated that blockade of LTαβ/LTβR interactions resulted in spleen and Peyer's patch development, but not lymph development [51]. Additional work by Koni et al. showed that complete absence of LTβ in mice translates in defective organization of peripheral lymph nodes, but not of mesenteric lymph nodes [52], while Banks et al. observed that LTα deficiency correlated with defective peripheral lymph nodes and Peyer's patches, but that some lymph node-like structures were found in the mesenteric fat [53]. In addition, Ettinger et al. showed a dose-dependent effect of blocking of LTβR in splenic development [51]. All of these data suggest differential signal requirements across secondary lymphoid organs, and that varying levels of cytokines results in fluctuating effects in lymphoid organization. It is

possible that in our model the downregulation of expression of LTβ and LTα is not enough to cause a defect in mesenteric or that other compensatory signal(s) unique to the mesenteric lymph are required. Furthermore, mesenteric lymph nodes are known to have constitutive germinal centers due in part to signals from the microbiota [54]. Given our data that indicate that STag induced IL-4 independent lymph node reorganization is at least partially dependent on IFNγ (Fig. 5A–C), it is plausible that commensal microbiota induction of cytokines is a mechanism behind the difference between the MIN and peripheral lymph nodes in steady state. In our model IFNγ blockade with a neutralizing antibody was able to reduce STag induced peripheral lymph node LEC expansion, but not FDC expansion, which suggests that while the two cell types have an equivalent requirement for IL-4 signaling, they differ in their dependence on IFNγ for antigen induced expansion. This raises the possibility that different stromal cell subsets may be regulated by different combinations of B and T-cell derived cytokines, a possibility that will be explored in future work. We also observed profoundly altered localization of B-cell follicles in IL-$4^{-/-}$ and 4getIL-$4R^{-/-}$ mice, an observation that is in agreement with previous reports that *K14-VEGFR-3-Ig* mice that lack lymphatic capillaries have disorganized B-cell zones in their peripheral lymph nodes [31], and supports the notion that stromal cells are critically important for maintaining peripheral lymph node homeostasis and lymphocyte positioning.

Our experiments also revealed a significant decrease in the number of FDC-$M2^{+}$ follicular dendritic cells in the absence of IL-4 signaling (Fig. 2B, C), and even more strikingly, a profound aberration in their localization within peripheral lymph nodes (Fig. 2F, G). In our model, the decreased number of follicular dendritic cells did not correlate with reduced B cell numbers in steady state or *Baff* transcript levels, suggesting that IL-4 influenced FDC activation or function does not compromise B-cell development. It is unclear whether other B-cell survival signals such as Bcl-2 or transcription factors of the NF-kB family, which have been shown as crucial for B cell [55] play a compensatory role in the maintenance of B cells. Interestingly, the aberrantly located FDCs colocalized with clusters of $B220^{+}$ B cells, raising the possibility that this FDC mal-positioning drives alterations to B-cell follicles, a possibility that is supported by published data that indicate FDCs and B cells maintain their positioning via a LTαβ-LTβR-positive feedback loop [56–58]. Nevertheless, the source of LTαβ in these studies remains unknown, and will be the focus of future studies. CXCL13 production is not altered in the absence of IL-4, suggesting that the traditional mechanisms underlying B-cell positioning are intact, and supports the possibility that the observed alterations in positioning are likely driven by inappropriate positioning of stromal cells. The relative contributions of FDCs versus LECs in governing B-cell positioning remains unclear, however, the data suggest that both of these stromal cell populations are responsive to both IL-4 (Figs. 1 and 2) and lymphotoxin [50, 59], and that alterations to either cell type alters B-cell follicle localization. This raises the possibility that LECs and FDCs work in concert to enforce peripheral lymph node organization.

Overall our data suggest a novel role for IL-4 in maintaining the lymphocyte stromal axis in peripheral lymph nodes both during steady state, and following antigen induced inflammation. This is due in part to IL-4 induced production of lymphotoxin-α and β, but it is likely that there are other molecular mechanisms involved in this regulation including a cell intrinsic role for IL-4 signaling in FDCs and LECs, and the mechanistic delineation of

the stromal cell intrinsic versus extrinsic roles of IL-4 will be the focus of future work. Our work used Stat-6 and IL-4Rα deficient mice to complement the findings from IL-4 deficient mice. Both of these strains would also be deficient in responding to IL-13. We looked for IL-13 expression at steady state, but were unable to detect significant transcripts of *il-13* in naïve peripheral lymph nodes on any genetic background (data not shown). While this is not conclusive, it suggests that physiological relevance is unlikely in our model. Future studies should strive to unequivocally determine the homeostatic role of IL-13 in the maintenance of stromal cell population in peripheral lymph nodes.

Our experiments found that a commercially available tetanus diphtheria vaccine failed to induce significant expansion of either FDC of LEC in IL-4Rα deficient mice. Furthermore, when we examined the cellular and humoral immune response to tetanus/diphtheria, we found that in the absence of IL-4 signaling, immunization fails to induce robust Tfh and germinal center formation and most significantly, fails to induce plasma cell differentiation. This is accompanied by significantly lower serum anti-diphtheria IgG1 titers, a finding that is likely to have clinical consequences. FDCs have previously been shown to important for the maintenance of memory B cells and long-term humoral immunity [60, 61] (via CD21/35), so these data fit within that paradigm. Ihe inability of IL-4Rα deficient mice to undergo lymph node reorganization following immunization with some Th2 antigens is particularly important because most commercially available vaccines are administered s.c. or i.m. and would drain to peripheral lymph nodes. Ihe majority of these formulations utilize aluminum salts as their adjuvants, and these compounds are known induce a strong Th2 response [62, 63]. The reduction in diphtheria, but not tetanus-specific responses suggests that individual antigens may have an intrinsic requirement for IL-4 induction regardless of the adjuvant that they are administered with. This possibility has significant implications for monitoring the efficacy of vaccine formulations with multiple antigens, and for understanding the molecular basis of immunization failure. A greater understanding of the role of cytokines like IL-4 and IFNγ in lymph node organization/reorganization may lead to rational approaches to promote long-term humoral immunity.

Materials and methods

Mice strains and in vivo treatments

C57BL/6J (WT), C57BL/6J IL-4$^{-/-}$, C57BL/6J STAT6$^{-/-}$ 4get homozygous (Jackson Laboratory), and 4get IL-4Rα$^{-/-}$ (gift from Markus Mohrs) were bred in-house under specific pathogen free (SPF) conditions at Purdue University. All experimental procedures with mice were approved by the Purdue Animal Care and Use Committee (PACUC). All experimental mice were a mix of female and male age-matched mice of approximately 6–8 weeks of age. For immunization experiments, SEA was prepared from isolated *Schistosoma mansoni* eggs as previously described [64, 65]. STag was prepared from culture-derived *Toxoplasma gondii* tachyzoites ([30] strain ME-49, kindly provided by William Sullivan). Thirty micrograms of either SEA or STag were injected s.c. in the rear footpad and mice were sacrificed 8-days postimmunization. Tetanus/Diphtheria commercial vaccine (Tetanus and Diphtheria Toxoids Adsorbed, MassBiologics) was injected s.c. in the rear footpad at ~1/10 the human dose. For IFN-γ blockade experiments, 200 μg of anti-IFN-γ (XMG1.2,

BioXcell [66] or isotype control (anti HRP, Clone: HRPN, BioXcell) was injected both s.c. and i.p. on days −3, 0, 1, 3, and 5.

Enzymatic digestion of popliteal lymph nodes

For flow cytometric analysis, collected pLN were digested with DMEM containing 1 mg/mL of Collagenase D (Sigma) and 0.1 mg/mL DNAse I (Invitrogen) as previously described [67, 68]. In short, digestion medium was injected in the center of the nodes and incubated at 37°C for 15 min, with occasional inversion to ensure the mixing of the contents. The digested nodes were filtered through a 100 μm cell strainer and cell suspensions were washed with 15 mL of DMEM. Following wash with DMEM, cells were centrifuged (1500 rpm, 5 min, 4°C), cells were resuspended to appropriate volume in FACS buffer (2% fetal calf serum, 5 mM EDTA in PBS), counted for cell numbers and used for flow cytometry staining.

Flow cytometry and antibodies

Surface staining and intracellular staining for single cell suspensions was performed as previously described [69]. Samples were acquired using a BD FACSCanto II and analyzed using FlowJo software (TreeStar, v.10.0.6). In brief, intracellular staining was performed by restimulation of cells for 5 h with PMA 50 ng/mL) and ionomycin (1 mg/mL) in the presence of brefeldin A (10 mg/mL) as described previously [70]. The following antibodies from BD, eBioscience, Bio-Legend, ImmunoKontact) conjugated with PE, PE-Cy5, PE-Cy7, allophycocyanin, allophycocyanin-Cy7, Pacific blue, or biotin) were used: CD4 (RM4-5), CD19 (1D3), CD138, (281-2), IgG1 (A85-1), IgD (11-26), CD11c (N418), F4/80 (BM8), GL7 (GL7), CD31 (390), podoplanin (eBIO 8.1.1), FDC-M2 (FDC-M2), CD21/35 (7G6), PD-1 (J43), CXCR5 (2G8), PNAd (MECA-79). IL-21R/FC chimera (R&D Systems; 596-MR-100) was used for detection of IL-21-producing cells. Secondary staining was performed using streptavidin-allophycocyanin or streptavidin allophycocyanin-Cy7. To reduce nonspecific binding, Fc-block (anti-mouse CD16/32 (clone 93)) was used in all flow cytometry experiments. Flow cytometry experiments were conducted in accordance to the “Guidelines for the use of flow cytometry and cell sorting in immunological studies” [71].

Immunofluorescence microscopy

The entire collected lymph node was placed in Tissue-Tek optimum cutting temperature compound (Thermo Scientific) and immediately frozen in liquid nitrogen. Serial cryostat sections (10 μm) were collected, air-dried, and fixed in ice-cold 75% acetone/25% ethanol for 5 min. Tissue was rehydrated in PBS for 10 min and blocked using biotin blocking kit (Vector Laboratories, according to manufacturer’s instructions) followed by incubation with 1% v/v in PBS of rat and rabbit serum. Immunofluorescence staining was performed overnight at 4°C with diluted antibodies in blocking buffer. Secondary staining was performed the following morning by incubating with specific antibodies for 1 hour at room temperature. Mounting was done using ProLong anti-fade reagents (Life Technologies) followed by imaging using Leica TCS Sp5 Laser Scanning Microscopy using tile scan feature with an average grid size of 3 × 3 taken with a 20x objective at a resolution of 1024 × 1024. Image postprocessing was done using Fiji is Just ImageJ software (1.47v).

RNA isolation and q-RT-PCR analysis

Whole collected lymph nodes were homogenized in Trizol™ and RNA isolation was performed as previously described [24, 72]. RNA was used for cDNA synthesis using Superscript II (Invitrogen) for qPCR analysis. qPCR for *Lt*β (Assay ID: Mm00434774_g1), *Lt*α (Assay ID: Mm00440228-gH), *Baff* (Assay ID: Mm00446347_m1), *ccl19* (Assay ID: Mm00839967_g1), *ccl21b* (Assay ID: Mm03646971_gH), and *cxcl13* (Assay ID: Mm00444533_m1) was performed using Taqman Gene expression assays with beta actin as the housekeeping gene (Assay ID: Mm02619580_g1). (ThermoFisher) on an Applied Biosystems StepOne Plus Real-Time PCR System.

Western blot

Total protein was isolated from naïve lymph nodes using Tissue extraction Reagent I (Invitrogen) and diluted in sample buffer. Thirty micrograms of protein was loaded to 15% SDS-PAGE gels and transferred to nitrocellulose membrane. Membranes were incubated with anti-lymphotoxin β antibody (Abcam, ab64835) and β-tubulin antibody (Santa Cruz, clone N-20) overnight and imaged using Odyssey infrared imaging system from LI-COR Biosciences.

ELISA

Tetanus- and diphtheria-specific IgG1 endpoint titers were determined by ELISA using the mAb X56 (BD) and Immulon 4HB plates (Thermo Fisher Scientific). Plates were coated overnight with tetanus (List Labs) and diphtheria with 2 μg/mL/well at 4°C, blocked with 1% milk and incubated with serial dilutions of sera, followed by incubation with anti-mouse IgG1 ads-HRP antibody and ABTS substrate. Plates were read at 405 nm at room temperature on a BioTek plate reader.

Quantification of Podoplanin/CD31 costained areas

To visualize and quantify the spatial distribution of areas costained with an antibody against podoplanin and a label identifying CD31, we used Euclidean distance map (EDM) analysis of locally bright features (LBF) following the methodology by Knowles et al. [36]. Briefly, the lymph node images were processed to produce a Boolean-and result of podoplanin and CD31 channel. The resultant greyscale images represent costained pixels. The images were further automatically threshold to LBFs. Separately, a ROI mapping the boundaries of the lymph nodes were established and converted into binary masks. The mask images were transformed to 16-bit greyscale EDMs. Finally, the EDM-LBF maps were created by multiplying the EDM images by the LBF maps. The results encoded the distances to the boundaries of ROIs as greyscale values. The quantitation was blinded and performed by two different researchers.

Statistical analysis

Statistical analyses were performed using either a nonparametric Mann-Whitney test, unpaired Student's *t* test or ANOVA, Bonferroni's multiple comparison test based on the distribution of the data. p values ≤ 0.05 were considered statistically significant. Graph generation and statistical analyses were performed using Prism (GraphPad v5.0). Cohen's d

was calculated for effect size based on between-group differences by using the means and standard deviation of two groups. Values >0.8 were considered a large effect [73].

Supplementary Material

Refer to Web version on PubMed Central for supplementary material.

Acknowledgments:

The authors thank Taylor Bailey for helpful discussions, Dr. Gwendalyn Randolph for confocal microscopy advice and helpful discussions, and Dr. William Sullivan for *Toxoplasma gondii* tachyzoites. K.C.F. conceived of the project, K.C.F. and D.C.S. designed the experiments, K.C.F., D.C.S., L.G., and A.R. performed experiments, K.C.F., D.C.S., A.R., and B.R. analyzed the data, K.C.F., D.C.S., and B.R. wrote the manuscript. The work was supported by Purdue University, a Scientist Development Grant from the American Heart Association to K.C.F. (14SDG18230012), a R01 (AI135045) to K.C.F. and an American Heart Association Award (18PRE34030086) to D.C.S.

Abbreviations:

BEC	blood endothelial cell
EDM	Euclidean distance map
FDC	follicular dendritic cell
FRC	fibroblastic reticular cell
HEV	High endothelial venule
LBF	locally bright features
LEC	lymphatic endothelial cell
ROI	region of interest
SLO	secondary lymphoid organs

References

1. Junt T, Scandella E and Ludewig B, Form follows function: lymphoid tissue microarchitecture in antimicrobial immune defence. Nat. Rev. Immunol 2008 8: 764–775. [PubMed: 18825130]
2. Ruddle NH and Akirav EM, Secondary lymphoid organs: responding to genetic and environmental cues in ontogeny and the immune response. J. Immunol 2009 183: 2205–2212. [PubMed: 19661265]
3. Klaus GG, Humphrey JH, Kunkl A and Dongworth DW, The follicular dendritic cell: its role in antigen presentation in the generation of immunological memory. Immunol. Rev 1980 53: 3–28.
4. Reynes M, Aubert JP, Cohen JH, Audouin J, Tricottet V, Diebold J and Kazatchkine MD, Human follicular dendritic cells express CR1, CR2, and CR3 complement receptor antigens. J. Immunol 1985 135: 2687–2694. [PubMed: 2411809]
5. Cremasco V, Woodruff MC, Onder L, Cupovic J, Nieves-Bonilla JM, Schildberg FA, Chang J et al., B cell homeostasis and follicle confines are governed by fibroblastic reticular cells. Nat. Immunol 2014 15: 973–981. [PubMed: 25151489]
6. Katakai T and Kinashi T, Microenvironmental control of high-speed interstitial T cell migration in the lymph node. Front Immunol. 2016 7: 194. [PubMed: 27242799]

7. Onder L, Narang P, Scandella E, Chai Q, Iolyeva M, Hoorweg K, Halin C et al., IL-7-producing stromal cells are critical for lymph node remodeling. Blood 2012 120: 4675–4683.
8. Farr AG, Berry ML, Kim A, Nelson AJ, Welch MP and Aruffo A, Characterization and cloning of a novel glycoprotein expressed by stromal cells in T-dependent areas of peripheral lymphoid tissues. J. Exp. Med 1992 176: 1477–1482. [PubMed: 1402691]
9. Luther SA, Tang HL, Hyman PL, Farr AG and Cyster JG, Coexpression of the chemokines ELC and SLC by T zone stromal cells and deletion of the ELC gene in the plt/plt mouse. Proc. Natl. Acad. Sci. USA 2000 97: 12694–12699. [PubMed: 11070085]
10. Kedl RM, Lindsay RS, Finlon JM, Lucas ED, Friedman RS and Tamburini BAJ, Migratory dendritic cells acquire and present lymphatic endothelial cell-archived antigens during lymph node contraction. Nat. Commun 20178: 2034. [PubMed: 29229919]
11. Onder L, Morbe U, Pikor N, Novkovic M, Cheng HW, Hehlgans T, Pfeffer K et al., Lymphatic endothelial cells control initiation of lymph node organogenesis. Immunity 201747: 80–92, e84. [PubMed: 28709801]
12. Onder L, Danuser R, Scandella E, Firner S, Chai Q, Hehlgans T, Stein JV et al., Endothelial cell-specific lymphotoxin-beta receptor signaling is critical for lymph node and high endothelial venule formation. J. Exp. Med 2013 210: 465–473. [PubMed: 23420877]
13. McCarthy DD, Summers-Deluca L, Vu F, Chiu S, Gao Y and Gommerman JL, The lymphotoxin pathway: beyond lymph node development. Immunol. Res 2006 35: 41–54. [PubMed: 17003508]
14. Ngo VN, Korner H, Gunn MD, Schmidt KN, Riminton DS, Cooper MD, Browning JL et al., Lymphotoxin alpha/beta and tumor necrosis factor are required for stromal cell expression of homing chemokines in B and T cell areas of the spleen. J. Exp. Med 1999 189: 403–412. [PubMed: 9892622]
15. Kain MJ and Owens BM, Stromal cell regulation of homeostatic and inflammatory lymphoid organogenesis. Immunology 2013 140: 12–21.
16. Kumar V, Dasoveanu DC, Chyou S, Tzeng TC, Rozo C, Liang Y, Stohl W et al., A dendritic-cell-stromal axis maintains immune responses in lymph nodes. Immunity 2015 42: 719–730. [PubMed: 25902483]
17. Vitetta ES, Ohara J, Myers CD, Layton JE, Krammer PH and Paul WE, Serological, biochemical, and functional identity of B cell-stimulatory factor 1 and B cell differentiation factor for IgG1. J. Exp. Med 1985 162: 1726–1731. [PubMed: 3932582]
18. Coffman RL, Ohara J, Bond MW, Carty J, Zlotnik A and Paul WE, B cell stimulatory factor-1 enhances the IgE response of lipopolysaccharide-activated B cells. J. Immunol 1986 136: 4538–4541. [PubMed: 3486902]
19. Mosmann TR, Bond MW, Coffman RL, Ohara J and Paul WE, T-cell andmast cell lines respond to B-cell stimulatory factor 1. Proc. Natl. Acad. Sci. USA 1986 83: 5654–5658. [PubMed: 3090545]
20. Brown MA and Hural J, Functions of IL-4 and control of its expression. Crit. Rev. Immunol 1997 17: 1–32. [PubMed: 9034722]
21. Pelly VS, Kannan Y, Coomes SM, Entwistle LJ, Ruckerl D, Seddon B, MacDonald AS et al., IL-4-producing ILC2s are required for the differentiation of TH2 cells following *Heligmosomoides polygyrus* infection. Mucosal Immunol. 2016 9: 1407–1417. [PubMed: 26883724]
22. Stetson DB, Mohrs M, Reinhardt RL, Baron JL, Wang ZE, Gapin L, Kronenberg M et al., Constitutive cytokine mRNAs mark natural killer (NK) and NK T cells poised for rapid effector function. J. Exp. Med 2003 198: 1069–1076. [PubMed: 14530376]
23. Nelms K, Keegan AD, Zamorano J, Ryan JJ and Paul WE, The IL-4 receptor: signaling mechanisms and biologic functions. Annu. Rev. Immunol 1999 17: 701–738. [PubMed: 10358772]
24. Heng TS, Painter MW and Immunological Genome Project C., The Immunological Genome Project: networks of gene expression in immune cells. Nat. Immunol 2008 9: 1091–1094. [PubMed: 18800157]
25. Kammer W, Lischke A, Moriggl R, Groner B, Ziemiecki A, Gurniak CB, Berg LJ et al., Homodimerization of interleukin-4 receptor alpha chain can induce intracellular signaling. J. Biol. Chem 1996 271: 23634–23637. [PubMed: 8798580]

26. Liang HE, Reinhardt RL, Bando JK, Sullivan BM, Ho IC and Locksley RM, Divergent expression patterns of IL-4 and IL-13 define unique functions in allergic immunity. Nat. Immunol 2011 13: 58–66. [PubMed: 22138715]
27. Takeda K, Tanaka T, Shi W, Matsumoto M, Minami M, Kashiwamura S, Nakanishi K et al., Essential role of Stat6 in IL-4 signalling. Nature 1996 380: 627–630.
28. Luzina IG, Keegan AD, Heller NM, Rook GA, Shea-Donohue T and Atamas SP, Regulation of inflammation by interleukin-4: a review of “alternatives”. J. Leukoc. Biol 2012 92: 753–764. [PubMed: 22782966]
29. Paul WE, Interleukin-4: a prototypic immunoregulatory lymphokine. Blood 1991 77: 1859–1870. [PubMed: 2018830]
30. Fairfax KC, Everts B, Amiel E, Smith AM, Schramm G, Haas H, Randolph GJ et al., IL-4-secreting secondary T follicular helper (Tfh) cells arise from memory T cells, not persisting Tfh cells, through a B cell-dependent mechanism. J. Immunol 2015 194: 2999–3010. [PubMed: 25712216]
31. Thomas SN, Rutkowski JM, Pasquier M, Kuan EL, Alitalo K, Randolph GJ and Swartz MA, Impaired humoral immunity and tolerance in K14-VEGFR-3-Ig mice that lack dermal lymphatic drainage. J. Immunol 2012 189: 2181–2190. [PubMed: 22844119]
32. Card CM, Yu SS and Swartz MA, Emerging roles of lymphatic endothelium in regulating adaptive immunity. J. Clin. Invest 2014 124: 943–952. [PubMed: 24590280]
33. Yeo KP and Angeli V, Bidirectional crosstalk between lymphatic endothelial cell and T cell and its implications in tumor immunity. Front Immunol. 2017 8: 83. [PubMed: 28220121]
34. Mueller SN and Germain RN, Stromal cell contributions to the homeostasis and functionality of the immune system. Nat. Rev. Immunol 2009 9: 618–629. [PubMed: 19644499]
35. Tamburini BA, Burchill MA and Kedl RM, Antigen capture and archiving by lymphatic endothelial cells following vaccination or viral infection. Nat. Commun 2014 5: 3989. [PubMed: 24905362]
36. Knowles DW, Sudar D, Bator-Kelly C, Bissell MJ and Lelievre SA, Automated local bright feature image analysis of nuclear protein distribution identifies changes in tissue phenotype. Proc. Natl. Acad. Sci. USA 2006 103: 4445–4450. [PubMed: 16537359]
37. van Buul JD, Kanters E and Hordijk PL, Endothelial signaling by Ig-like cell adhesion molecules. Arterioscler. Thromb. Vasc. Biol 2007 27: 1870–1876. [PubMed: 17585068]
38. Moussion C and Girard JP, Dendritic cells control lymphocyte entry to lymph nodes through high endothelial venules. Nature 2011 479: 542–546.
39. Aguzzi A, Kranich J and Krautler NJ, Follicular dendritic cells: origin, phenotype, and function in health and disease. Trends Immunol. 2014 35: 105–113. [PubMed: 24315719]
40. El Shikh ME and Pitzalis C, Follicular dendritic cells in health and disease. Front Immunol. 2012 3: 292. [PubMed: 23049531]
41. Allen CD and Cyster JG, Follicular dendritic cell networks of primary follicles and germinal centers: phenotype and function. Semin. Immunol 2008 20: 14–25.
42. Bajenoff M, Egen JG, Koo LY, Laugier JP, Brau F, Glaichenhaus N and Germain RN, Stromal cell networks regulate lymphocyte entry, migration, and territoriality in lymph nodes. Immunity 2006 25: 989–1001. [PubMed: 17112751]
43. Zhou YW, Aritake S, Tri Endharti A, Wu J, Hayakawa A, Nakashima I and Suzuki H, Murine lymph node-derived stromal cells effectively support survival but induce no activation/proliferation of peripheral resting T cells in vitro. Immunology 2003 109: 496–503. [PubMed: 12871215]
44. Zindl CL, Kim TH, Zeng M, Archambault AS, Grayson MH, Choi K, Schreiber RD et al., The lymphotoxin LTalpha(1)beta(2) controls postnatal and adult spleen marginal sinus vascular structure and function. Immunity 2009 30: 408–420. [PubMed: 19303389]
45. Chen X, Ma W, Zhang T, Wu L and Qi H, Phenotypic Tfh development promoted by CXCR5-controlled re-localization and IL-6 from radiation-resistant cells. Protein Cell 2015 6: 825–832. [PubMed: 26404031]
46. Pandey S, Mourcin F, Marchand T, Nayar S, Guirriec M, Pangault C, Monvoisin C et al., IL-4/CXCL12 loop is a key regulator of lymphoid stroma function in follicular lymphoma. Blood 2017 129: 2507–2518. [PubMed: 28202459]

47. Sellers RS, Clifford CB, Treuting PM and Brayton C, Immunological variation between inbred laboratory mouse strains: points to consider in phenotyping genetically immunomodified mice. Vet. Pathol 2012 49: 32–43. [PubMed: 22135019]
48. Mills CD, Kincaid K, Alt JM, Heilman MJ and Hill AM, M-1/M-2 macrophages and the Th1/Th2 paradigm. J. Immunol 2000 164: 6166–6173. [PubMed: 10843666]
49. Furtado GC, Marinkovic T, Martin AP, Garin A, Hoch B, Hubner W, Chen BK et al., Lymphotoxin beta receptor signaling is required for inflammatory lymphangiogenesis in the thyroid. Proc. Natl. Acad. Sci. USA 2007 104: 5026–5031. [PubMed: 17360402]
50. Dubey LK, Lebon L, Mosconi I, Yang CY, Scandella E, Ludewig B, Luther SA et al., Lymphotoxin-dependent B cell-FRC crosstalk promotes de novo follicle formation and antibody production following intestinal Helminth infection. Cell Rep. 2016 15: 1527–1541.
51. Ettinger R, Browning JL, Michie SA, van Ewijk W and McDevitt HO, Disrupted splenic architecture, but normal lymph node development in mice expressing a soluble lymphotoxin-beta receptor-IgG1 fusion protein. Proc. Natl. Acad. Sci. USA 1996 93: 13102–13107. [PubMed: 8917551]
52. Koni PA, Sacca R, Lawton P, Browning JL, Ruddle NH and Flavell RA, Distinct roles in lymphoid organogenesis for lymphotoxins alpha and beta revealed in lymphotoxin beta-deficient mice. Immunity 1997 6: 491–500. [PubMed: 9133428]
53. Banks TA, Rouse BT, Kerley MK, Blair PJ, Godfrey VL, Kuklin NA, Bouley DM et al., Lymphotoxin-alpha-deficient mice. Effects on secondary lymphoid organ development and humoral immune responsiveness. J. Immunol 1995 155: 1685–1693. [PubMed: 7636227]
54. Round JL and Mazmanian SK, The gut microbiota shapes intestinal immune responses during health and disease. Nat. Rev. Immunol 2009 9: 313–323. [PubMed: 19343057]
55. Gerondakis S and Strasser A, The role of Rel/NF-kappaB transcription factors in B lymphocyte survival. Semin. Immunol 2003 15: 159–166. [PubMed: 14563114]
56. Boulianne B, Porfilio EA, Pikor N and Gommerman JL, Lymphotoxin-sensitive microenvironments in homeostasis and inflammation. Front Immunol. 2012 3: 243. [PubMed: 22866054]
57. Mackay F, Majeau GR, Lawton P, Hochman PS and Browning JL, Lymphotoxin but not tumor necrosis factor functions to maintain splenic architecture and humoral responsiveness in adult mice. Eur. J. Immunol 1997 27: 2033–2042. [PubMed: 9295042]
58. Ansel KM, Ngo VN, Hyman PL, Luther SA, Forster R, Sedgwick JD, Browning JL et al., A chemokine-driven positive feedback loop organizes lymphoid follicles. Nature 2000 406: 309–314.
59. Chaplin DD and Fu Y, Cytokine regulation of secondary lymphoid organ development. Curr. Opin. Immunol 1998 10: 289–297. [PubMed: 9638365]
60. Ahearn JM, Fischer MB, Croix D, Goerg S, Ma M, Xia J, Zhou X et al., Disruption of the Cr2 locus results in a reduction in B-1a cells and in an impaired B cell response to T-dependent antigen. Immunity 1996 4: 251–262. [PubMed: 8624815]
61. Fang Y, Xu C, Fu YX, Holers VM and Molina H, Expression of complement receptors 1 and 2 on follicular dendritic cells is necessary for the generation of a strong antigen-specific IgG response. J. Immunol 1998 160: 5273–5279. [PubMed: 9605124]
62. Lindblad EB, Aluminium adjuvants—in retrospect and prospect. Vaccine 2004 22: 3658–3668. [PubMed: 15315845]
63. Brewer JM, (How) do aluminium adjuvants work? Immunol. Lett 2006 102: 10–15.
64. MacDonald AS, Patton EA, La Flamme AC, Araujo MI, Huxtable CR, Bauman B and Pearce EJ, Impaired Th2 development and increased mortality during *Schistosoma mansoni* infection in the absence of CD40/CD154 interaction. J. Immunol 2002 168: 4643–4649. [PubMed: 11971013]
65. Taylor JJ, Krawczyk CM, Mohrs M and Pearce EJ, Th2 cell hyporesponsiveness during chronicmurine schistosomiasis is cell intrinsic and linked to GRAIL expression. J. Clin. Invest 2009 119: 1019–1028. [PubMed: 19258704]
66. Choi YS, Gullicksrud JA, Xing S, Zeng Z, Shan Q, Li F, Love PE et al., LEF-1 and TCF-1 orchestrate T(FH) differentiation by regulating differentiation circuits upstream of the transcriptional repressor Bcl6. Nat. Immunol 2015 16: 980–990. [PubMed: 26214741]

67. Ng CT, Nayak BP, Schmedt C and Oldstone MB, Immortalized clones of fibroblastic reticular cells activate virus-specific T cells during virus infection. Proc. Natl. Acad. Sci. USA 2012 109: 7823–7828. [PubMed: 22550183]

68. Hara T, Shitara S, Imai K, Miyachi H, Kitano S, Yao H, Tani-ichi S et al., Identification of IL-7-producing cells in primary and secondary lymphoid organs using IL-7-GFP knock-in mice. J. Immunol 2012 189: 1577–1584. [PubMed: 22786774]

69. Glatman Zaretsky A, Taylor JJ, King IL, Marshall FA, Mohrs M and Pearce EJ, T follicular helper cells differentiate from Th2 cells in response to helminth antigens. J. Exp. Med 2009 206: 991–999. [PubMed: 19380637]

70. Everts B, Hussaarts L, Driessen NN, Meevissen MH, Schramm G, van der Ham AJ, van der Hoeven B et al., Schistosome-derived omega-1 drives Th2 polarization by suppressing protein synthesis following internalization by the mannose receptor. J. Exp. Med 2012209: 1753–1767, S1751. [PubMed: 22966004]

71. Cossarizza A, Chang HD, Radbruch A, Akdis M, Andra I, Annunziato F, Bacher P et al., Guidelines for the use of flow cytometry and cell sorting in immunological studies. Eur. J. Immunol 2017 47: 1584–1797. [PubMed: 29023707]

72. Fairfax KC, Everts B, Smith AM and Pearce EJ, Regulation of the development of the hepatic B cell compartment during Schistosoma mansoni infection. J. Immunol 2013 191:4202–4210. [PubMed: 24038090]

73. Cohen J, A power primer. Psychol. Bull 1992 112: 155–159. [PubMed: 19565683]

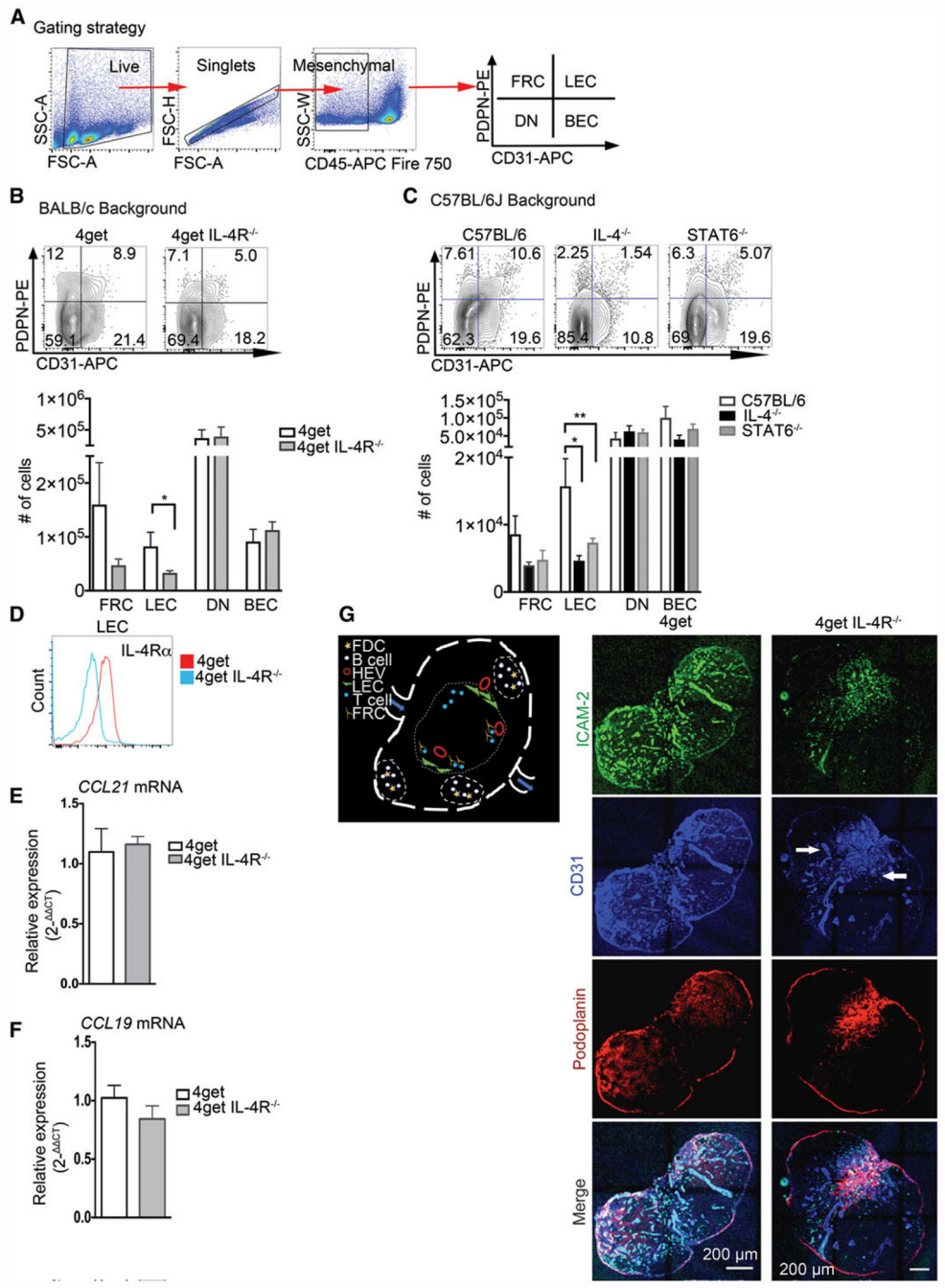

Figure 1.

Maintenance of endothelial cells in peripheral lymph nodes in steady state requires IL-4 signaling. C57BL/6J, IL-4KO, STAT6KO, 4get homozygous, and 4get IL-4RαKO mice were sacrificed at 6–8 weeks of age, and popliteal lymph nodes were collected, digested, and single cell suspensions were obtained and analyzed by flow cytometry for expression of indicated markers. Alternatively, intact popliteal lymph nodes were collected, frozen in optimum cutting temperature (OCT) medium, sectioned, and tile scans were acquired with a laser scanning confocal microscope. (A) Gating strategy for lymphatic endothelial cells (B)

Popliteal lymph node lymphatic endothelial cells from $CD45^-$ population (defined as $PDPN^+CD31^+$), BEC (defined as $CD31^+PDPN^-$), FRC ($PDPN^+$, $CD31^-$), and DN in 4get homozygous (control) and 4get IL-4RKO mice and (C) in C57BL/6J (control) and IL-4KO and STAT6KO in popliteal lymph node, error bar denotes mean ± SEM. (D) Expression of IL-4Rα in lymphatic endothelial cells from popliteal lymph node determined by flow cytometry. (E and F) Relative expression of CCL21 and CCL19 by quantitative PCR, respectively from naïve popliteal lymph nodes normalized to naïve 4get (control), bars show mean ± SEM. (G) Schematic of lymph node showing cells of interest in B-cell follicles and T-cell area. (H) Popliteal lymph node cryosections were stained for ICAM-2, green; CD31, blue and podoplanin, red. Scale bar: 200 μm. Arrowhead denotes CD31+ endothelial cells clusters preferentially localized in the medulla. Student *t*-test was used to determine statistical significance $*p < 0.05$, $**p < 0.01$. FACS data shown are concatenated from 3–5 mice per group and experiments were performed 3–4 times. Confocal images are representative of three different experiments with three mice per group.

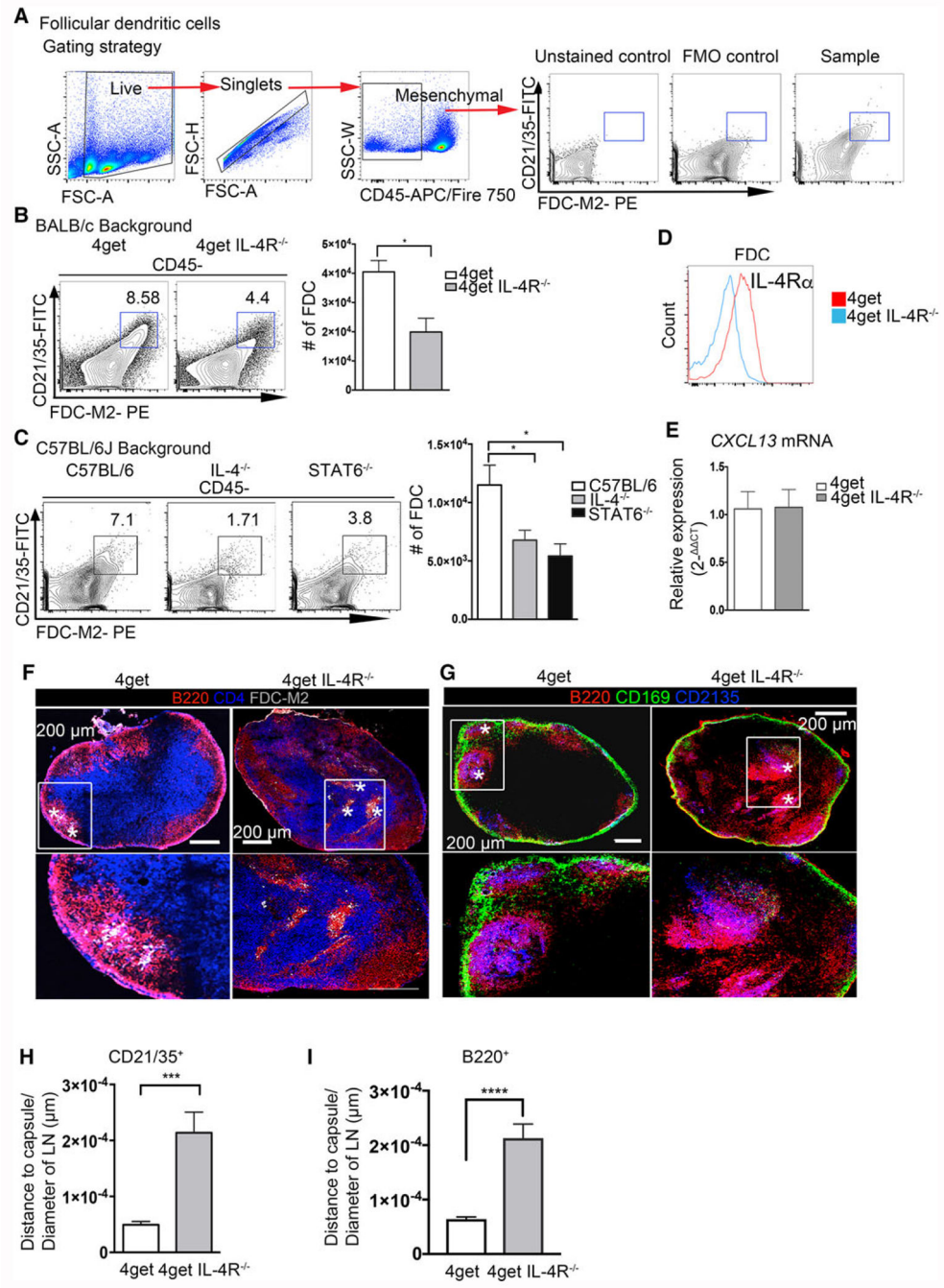

Figure 2.

IL-4 is required for proper follicular dendritic cell and B-cell follicle organization in peripheral lymph nodes in steady-state. Lymph nodes from naïve C57BL/6J, IL-4KO, STAT6KO, 4get homozygous, and 4get IL-4RαKO mice were digested with collagenase and smashed through a cell strainer to be analyzed by flow cytometry or frozen in OCT medium, and tile scans of cryosections were acquired with a laser scanning confocal microscope. (A) Gating strategy and staining controls. (B) Follicular dendritic cells ($CD21/35^{+}$ $FDC\text{-}M2^{+}$) gated from $CD45^{-}$ obtained from 4get homozygous and 4get IL-4Rα KO popliteal lymph

nodes and (C) popliteal lymph nodes of C57BL/6J, IL-4KO, and STAT6KO mice. (D) Expression of IL-4Rα in follicular dendritic cells from naïve popliteal lymph node. (E) Relative expression of CXCL13 from naïve pLNs, normalized to naïve 4get (control) bars show mean ± SEM. (F) Frozen popliteal lymph node sections from 4get homozygous (control) and 4get IL-4RαKO mice were stained for B220 (red), CD4 (blue), and FDC-M2 (gray). (G) Sections were stained for CD21/35 (blue, follicular dendritic cells), B220 (red, B cells), and CD169 (green, subcapsular macrophages). Asterisk denotes FDC-M2$^+$ cells and CD21/35$^+$ cells, scale bar: 200 μm. (H) Quantification of the distance of CD21/35$^+$ FDC to the LN capsule normalized to the LN diameter. (I) Quantification of B220$^+$ cells from the lymph node capsule and normalized to the total lymph node area. Bar depicts mean ± SEM. Image is representative of two independent experiments with 3–4 mice per group. FACS data shown are representative from 3–5 mice per group from three independent experiments. Confocal microscopy images are representative of 3–4 mice per group of three independent experiments. *$p < 0.05$, ***$p < 0.001$; statistical significance was calculated by unpaired Student's *t*-test.

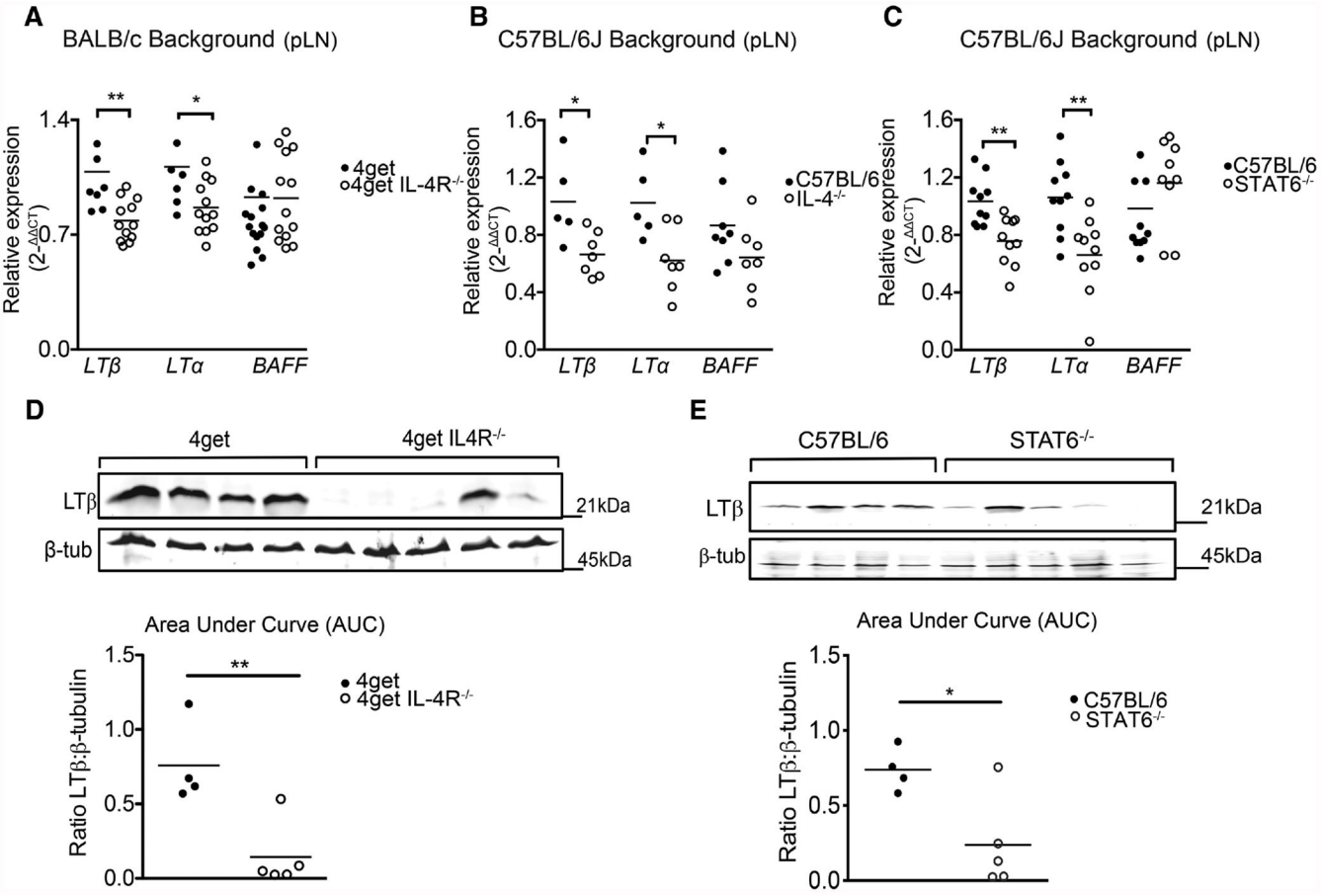

Figure 3.

LTβ and LTα mRNA levels in peripheral lymph nodes are dependent on the IL-4 signaling pathway in steady-state. 4get homozygous and 4get IL-4RαKO, as well as C57BL/6J and IL-4KO and STAT6KO mice were sacrificed at 6–9 weeks of age and popliteal lymph nodes were collected. Total RNA extracted using Trizol isolation followed by cDNA synthesis and quantitative expression of gene levels by q-RT-PCR. (A) Relative expression of LTβ, LTα, and BAFF normalized to beta-actin in 4get homozygous and 4get IL-4RKO mice. (B) Relative expression of LTα and LTβ and BAFF in whole popliteal lymph nodes from C57BL/6J and STAT6$^{-/-}$ and (C) C57BL/6J and IL-4KO mice. (D) LTβ protein expression normalized to β-tubulin in WT and 4get IL4RαKO mice. (E) LTβ protein expression normalized to β-tubulin in WT and STAT6KO mice. Statistical significance was determined by Man–Whitney test *$p < 0.05$, **$p < 0.01$. Data points represent individual mice. Quantitative PCR data represents three different experiments with $n > 4$ mice/group. Western blot data are representative of two independent experiments with $n \geq 4$ mice per group.

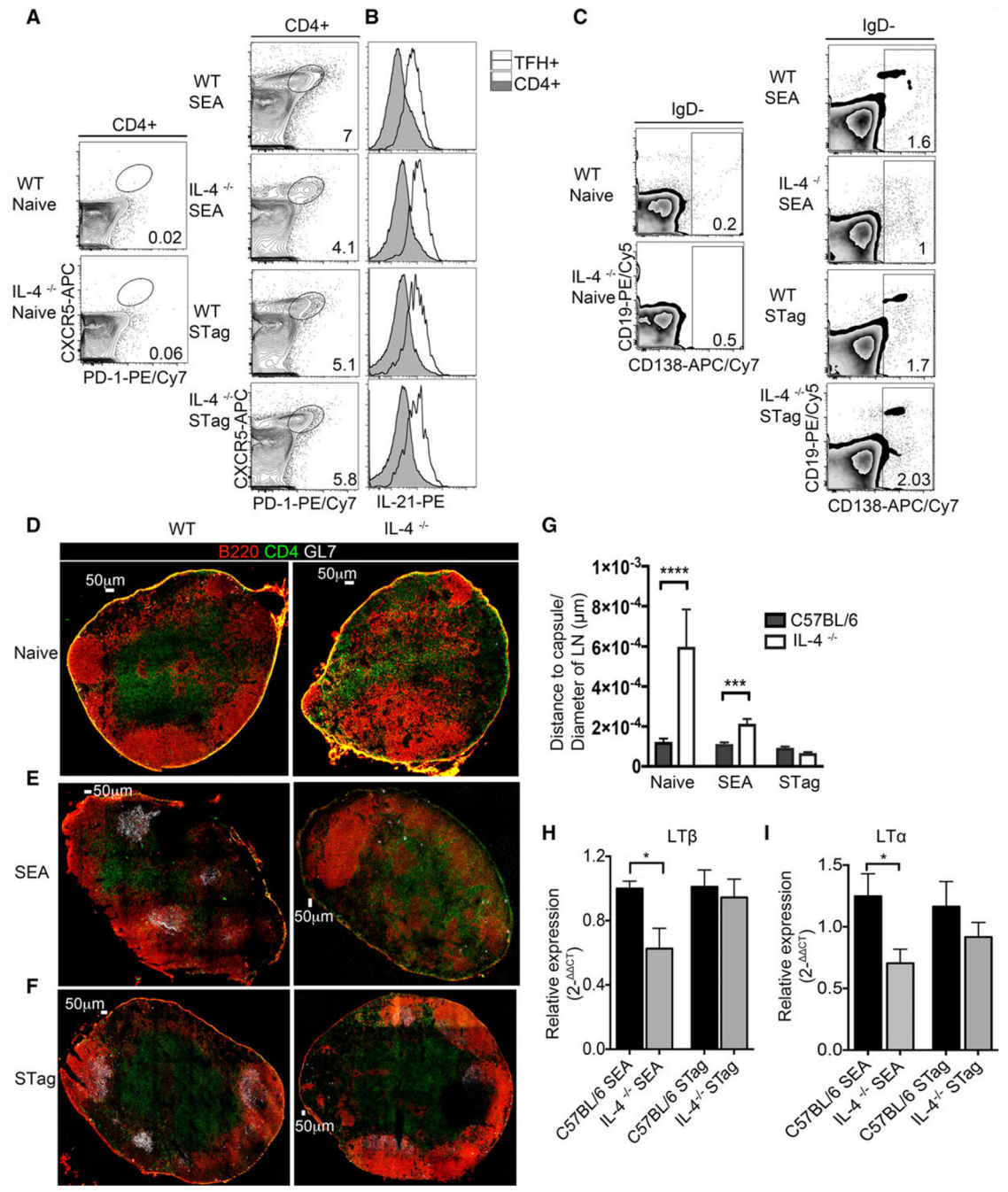

Figure 4.

IL-4 is required for lymph node reorganization and germinal center formation following immunization with SEA, but not STag antigens. C57BL/6J and IL-4KOmice were immunized s.c. in the footpad with either SEA or STag and draining and nondraining lymph nodes collected 8-days post-immunization. Lymph nodes were used to obtain single cell suspension for flow cytometry or frozen in OCT medium and section for imaging by confocal microscopy. (A) Frequency of T-follicular helper cells ($CD4^+$ $CXCR5^+PD\text{-}1^+$) in WT mice and IL-4KO from naïve or immunized with either SEA or STag. (B) Expression of

IL-21 in TFH^+ and $CD4^+$ cells from WT mice and IL-4KO immunized with either SEA or Stag. (C) Plasma cells ($CD19^{+/-}$ and $CD138^+$) pregated on IgD^- cells. (D) Cryosections of popliteal lymph node of naïve WT (C56BL/6J) and IL-4KO mice stained with B220 (red) GL7 (gray), CD4 (green), scale bar: 50 μm. (E) Frozen sections from SEA immunized WT (C57BL/6J) and IL-4KO mice stained for B220 (red) GL7 (gray), CD4 (green). (F) Frozen sections of popliteal lymph nodes from STag immunized C57BL/6J and IL-4KO mice stained for B220 (red) GL7 (gray), CD4 (green). Scale bar: 50 μm. (G) Quantitation of the distance of $B220^+$ expression to the capsule of lymph nodes normalized to lymph node area, bar show mean ± SEM. Data representative from three to five mice per group. (H) Relative gene expression of LTβ (normalized to β-actin) in SEA and STag immunized mice. (I) Relative expression of LTα (normalized to β-actin) in SEA and Stag immunized mice. FACS data depict concatenated samples and confocal images shown are representative of 3–5 mice. Data are representative of four independent experiments. Unpaired Student's *t* test was used to determine statistical significance; $*p < 0.05$, $***p < 0.001$, $***p < 0.0001$.

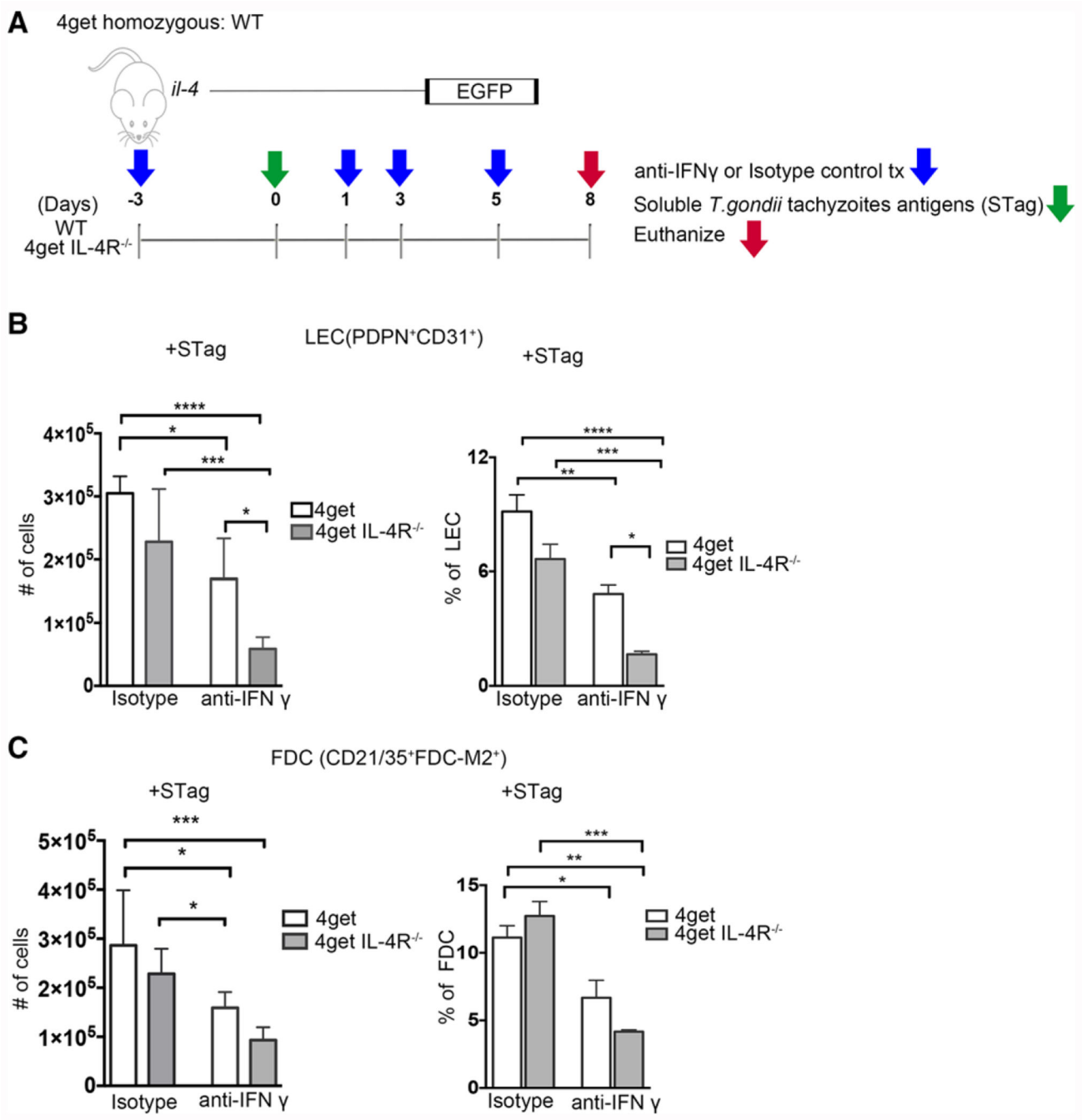

Figure 5.

IFN-γ promotes Stag induced LEC cell expansion in peripheral lymph nodes in the absence of IL-4Rα. 4get homozygous and 4get IL-4RαKO mice were immunized s.c. in the footpad with STag and treated with either anti-IFNγ or isotype control. Reactive popliteal lymph nodes were collected and single cell suspensions obtained and analyzed by flow cytometry. (A) Schematic of Stag immunization and blocking antibody treatment. (B) Cell numbers of lymphatic endothelial cells ($PDPN^+CD31^+$) in WT and knockout mice after treatment with isotype control or IFNγ blocking antibody, bars shown mean ± SEM. (C) Number of

follicular dendritic cells (FDC-M2^{+}CD21/35^{+}) from isotype and IFNγ blocking antibody treated WT and knockout mice were analyzed by flow cytometry. Bars shown mean ± SEM, *$p < 0.05$, **$p < 0.01$, ***$p < 0.001$, ****$p < 0.0001$ (ANOVA, Bonferroni's multiple comparison test). FACS data shown are concatenated from 3–6 mice per group, results are from two independent experiments.

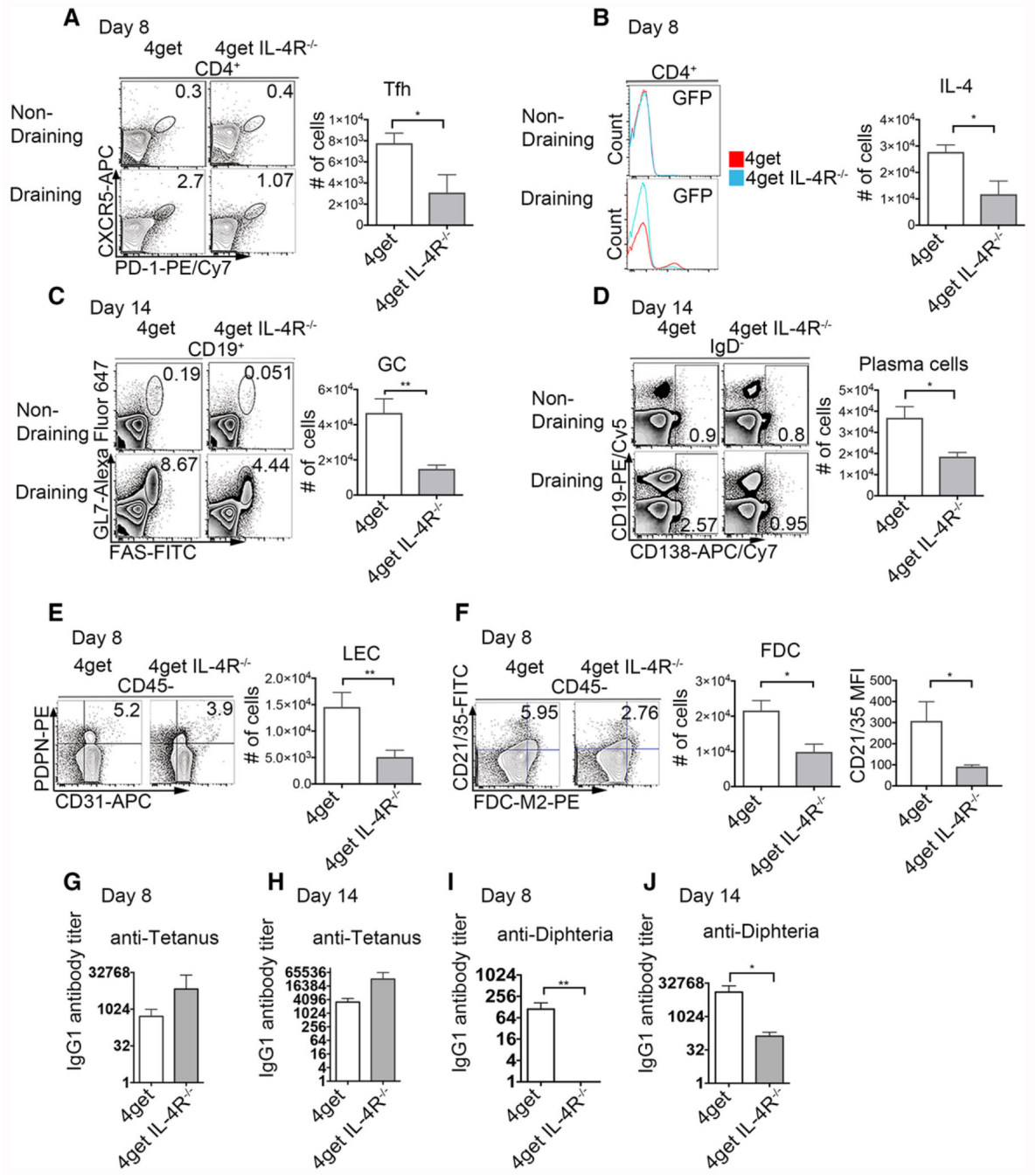

Figure 6.

Immunization with Tetanus/Diphtheria (TD) fails to induce Tfh expansion or a diphtheria-specific antibody response in mice lacking IL-4Rα. 4get homozygous and 4get IL-4RαKO mice were injected s.c. with 1/10 of the TD (with alum as adjuvant) dose employed in humans. Eight and 14 days postimmunization reactive peripheral lymph nodes were collected, digested, and filtered through a cell strainer to obtain a single cell suspension. Cells were stained with surface antibodies and analyzed by flow cytometry. (A) Expression and cell number of T-follicular helper cells ($CD4^+CXCR5^+PD\text{-}1^+$) at day 8 from

nondraining and reactive popliteal lymph nodes, bar denotes mean ± SEM (B) expression of IL-4 (GFP+) 8 days postimmunization with Tetanus diphtheria (C) Germinal center ($CD19^+GL7^+FAS^+$) at day 14, (D) Plasma cells and plasmablasts ($CD19^{+/-}$ $CD138^+$) at day 14 postimmunization pregated on IgD- (E) Lymphatic endothelial cells ($PDPN^+CD31^+$) at day 8 and (F) Follicular dendritic cells ($FDCM2^+CD21/35^+$) pregated on CD45 negative, cell numbers, and MFI, mean ± SEM. (G) Tetanus-specific IgG1 antibody titers at days 8 and (H) 14 postimmunization. (I) Diphtheria-specific IgG1 antibody titers at days 8 and (I) 14 postimmunization. FACS data represents concatenated samples from >3 mice per group and representative of three independent experiments for day 14 and two independent experiments for day 8. *$p < 0.05$, **$p < 0.01$; unpaired Student's t-test.